Rheol Acta
DOI 10.1007/s00397-016-0939-2

ORIGINAL CONTRIBUTION

A hierarchical multi-mode MSF model for long-chain branched polymer melts part III: shear flows

Esmaeil Narimissa[1] · **Manfred H. Wagner**[1]

Received: 21 January 2016 / Revised: 25 April 2016 / Accepted: 26 April 2016

Abstract A novel hierarchical multi-mode molecular stress function (HMMSF) model for long-chain branched (LCB) polymer melts is proposed, which implements the basic ideas of (i) the pom-pom model, (ii) hierarchal relaxation, (iii) dynamic dilution, (iv) interchain pressure and (v) convective constraint release relaxation mechanism. Here, the capability of this approach is demonstrated in modelling the steady shear data of a broadly distributed long-chain branched polymer melt with only two non-linear parameters, a dilution modulus and a convective constraint release (CCR) parameter.

Keywords Molecular stress function theory · Polymer melt · Hierarchical multi-mode MSF model · Shear flow · Convective Constraint Release

Introduction

Rheology is the study of material deformation and flow under the effect of stress. The importance of the relationship between the molecular structure and rheological behaviour of polymeric systems is due to the considerable sensitivity of the rheological properties to the structural ones, as well as the principal role of the rheological characteristics in flow behaviour during the melt processing of the polymers (Dealy and Larson 2006). The recent developments of quantitative mathematical models to analyse molecular structures through rheological properties have led to the evolution of the molecular structural aspects through rheological measurements, and vice versa, the prediction of the rheological aspects when the molecular structure is understood. The integration of the rheological modelling into the polymerization reactions and melt forming operations can result in the prediction of the detailed molecular structure of polymers, prediction of the rheological properties based on the structure, and the prediction of the detailed processing behaviour of polymers via numerical flow simulation techniques based on quantified rheological parameters (Dealy and Larson 2006). Therefore, the significance of the rheological modelling of polymeric systems has encouraged us to develop a comprehensive constitutive model capable of the prediction of rheological behaviours of long-chain branched (LCB) polymers for different categories of flow, i.e. uniaxial extensional, multiaxial extensional and shear deformations.

In part I of this research series (Narimissa et al. 2015), we introduced a novel hierarchical multi-mode molecular stress function (HMMSF) model for LCB polymers, which implements the basic ideas of the pom-pom model, hierarchal relaxation, dynamic dilution and the interchain pressure. This model accurately predicts the uniaxial extensional viscosity of several long-chain branched polymer melts based on their linear-viscoelastic characterization, and features only a single non-linear material parameter, the dilution modulus G_D.

In part II of this research (Narimissa et al. 2016), we presented the successful prediction of equibiaxial and planar (multiaxial) extensional viscosities of a LCB polymer through the implementation of the HMMSF model.

✉ Esmaeil Narimissa
esmaeil.narimissa@tu-berlin.de

[1] Polymer Engineering/Polymer Physics, Berlin Institute of Technology (TU Berlin), Fasanenstrasse 90, 10623 Berlin, Germany

Published online: 05 May 2016

The objective of this research is to apply, and if necessary, to modify the current version of the HMMSF model to predict the flow behaviour of LCB melt in steady shear flow.

Hierarchical multi-mode MSF model

The detailed developing steps and the theoretical discussions behind our hierarchical multi-mode molecular stress function (HMMSF) model are described elsewhere (Narimissa et al. 2015). The extra stress tensor of the HMMSF model is given as

$$\sigma(t) = \sum_i \int_{-\infty}^{+\infty} \frac{\partial G_i(t - t')}{\partial t'} f_i^2(t,t') \mathbf{S}_{\mathrm{DE}}^{\mathrm{IA}}(t,t') dt' \quad (1)$$

$\mathbf{S}_{\mathrm{DE}}^{\mathrm{IA}}(t,t')$ is the Doi and Edwards (DE) tensor assuming an independent alignment (IA) of tube segments (Doi and Edwards 1986), and $f_i(t,t')$represents the molecular stress functions of each mode i characterized by the partial relaxation moduli $G_i(t)$. The molecular stress functions $f_i(t,t')$ are inverse proportional to the relative tube diameter (Narimissa et al. 2015). The relaxation modulus $G(t)$ of the multi-mode pom-pom model can be represented by discrete Maxwell modes with partial relaxation moduli g_j and relaxation times τ_j,

$$G(t) = \sum_{j=1}^{n} G_j(t) = \sum_{j=1}^{n} g_j \exp(-t / \tau_j) \quad (2)$$

We distinguish between two dilution processes: 'permanent dilution' and 'dynamic dilution'. Permanent dilution occurs due to the presence of oligomeric chains and un-entangled or marginally entangled (fluctuating) chain ends. Dynamic dilution refers to the dynamic dilation of the tube diameter of the non-relaxed chains through the solvent effect of the already relaxed ones, which does not only affect the linear-viscoelastic properties but has also an effect on chain stretch, due to the dilation of the tube diameter. The onset of dynamic dilution occurs when the relaxation process has reached the dilution modulus $G_{\mathrm{D}} \leq G_{\mathrm{N}}^0$. As outlined by (Narimissa et al. 2015), the dilution modulus is a free parameter of the model, which needs to be fitted to non-linear-viscoelastic experimental evidence, since the mass fraction of oligomeric chains and un-entangled or marginally entangled chain ends is not known a priori. The mass fraction w_i of a dynamically diluted chain segment with relaxation time $\tau_i > \tau_D$ is determined by considering the ratio of the relaxation modulus at time $t=\tau_i$ to the dilution modulus $G_{\mathrm{D}}=G(t=\tau_{\mathrm{D}})$, while chain segments characterized by relaxation times $\tau_i<\tau_D$ are considered to be permanently diluted, and their weight fractions are fixed at $w_i=1$,

$$w_i^2 = \frac{G(t=\tau_i)}{G_{\mathrm{D}}} = \frac{1}{G_{\mathrm{D}}} \sum_{j=1}^{n} g_j \exp(-\tau_i / \tau_j) \quad \begin{matrix} \text{for } \tau_i > \tau_D \\ \text{for } \tau_i < \tau_D \end{matrix}$$
$$w_i^2 = 1 \quad (3)$$

It is assumed that the value of w_i obtained at $t=\tau_i$ can be attributed to the pom-pom with relaxation time τ_i. The evolution equation for the molecular stress function of each mode is given as,

$$\frac{\partial f_i}{\partial t} = f_i(\mathbf{K}:\mathbf{S}) - \frac{f_i - 1}{\tau_i}\left(1 - \frac{2}{3}w_i^2\right) - \frac{2}{3}\frac{f_i^2\left(f_i^3-1\right)}{3\tau_i} w_i^2 \quad (4)$$

Here, $\mathbf{K}$ is the deformation rate tensor, $\mathbf{S}$ the second order orientation tensor, and $f_i(\mathbf{K}:\mathbf{S})$ is the average increase of length per unit length of a tube segment with the starting conditions $f_i(t=t',t)=1$.The second term on the right hand side models stretch relaxation along the backbone tube, and the third term takes into account the interchain pressure perpendicular to the tube direction. The interchain pressure is reduced by tube dilation, which is caused by dilution of the chain segments as characterized by the fractions w_i defined in Eq. 3.

Thus, the HMMSF model consists of the multi-mode stress equation, a set of evolution equations for the molecular stresses f_i, and a hierarchical procedure to evaluate the effect of dynamic dilution with only one free non-linear parameter, the dilution modulus G_{D}.

Comparison between HMMSF model and experimental shear data

The shear rheological modellings of this study were conducted on a low density polyethylene (Lupolen 1810H) melt previously characterized and tested by Kraft (Kraft 1996) and Bastian (Bastian 2001; Wagner et al. 2001). Table 1 displays the weight average molecular weight (M_{w}), number average molecular weight (M_{n}), polydispersity index ($M_{\mathrm{w}}/M_{\mathrm{n}}$), melting temperature ($T_{\mathrm{m}}$), room temperature density (ρ_{RT}), testing temperature density (ρ_{T}), zero shear viscosity at testing temperature (η_0), melt flow index (MFI), activation energy (E_{a}), dilution modulus G_{D} obtained by modelling of the extensional data, and the linear-viscoelastic relaxation spectrum of Lupolen 1810H at testing temperature, 150 °C.

The steady shear rheological measurements of LDPE were conducted by Kraft (Kraft 1996) and Bastian (Bastian 2001; Wagner et al. 2001) through cone-and-plate configuration (0.1 rad gap angle) in strain-controlled rheometers (RMS

Table 1 Characterization of LDPE

Characteristics	LDPE	
Product	Lupolen 1810H	
Producer	BASF	
M_w (g/mol)	188,000	
M_n (g/mol)	16,600	
M_w/M_n	11.3	
T_m (°C)	110	
T (°C)	150	
ρ_{RT} (g/cm^3)	0.917	
ρ_T (g/cm^3)	0.778	
η_0 (@ T) (kPa.s)	65	
MFI (g/10 min)	1.2	
E_a (kJ/mol)	58.6	
G_D (Pa)	1.4×10^4	
Rheometer	RMS 800	
Relaxation spectrum at T		
i	g_i (Pa)	τ_i (s)
1	3.000E − 01	5.0E + 03
2	4.587E + 00	1.0E + 03
3	2.746E + 02	1.0E + 02
4	2.578E + 03	1.0E + 01
5	9.797E + 03	1.0E + 00
6	2.968E + 04	1.0E − 01
7	5.202E + 04	1.0E − 02

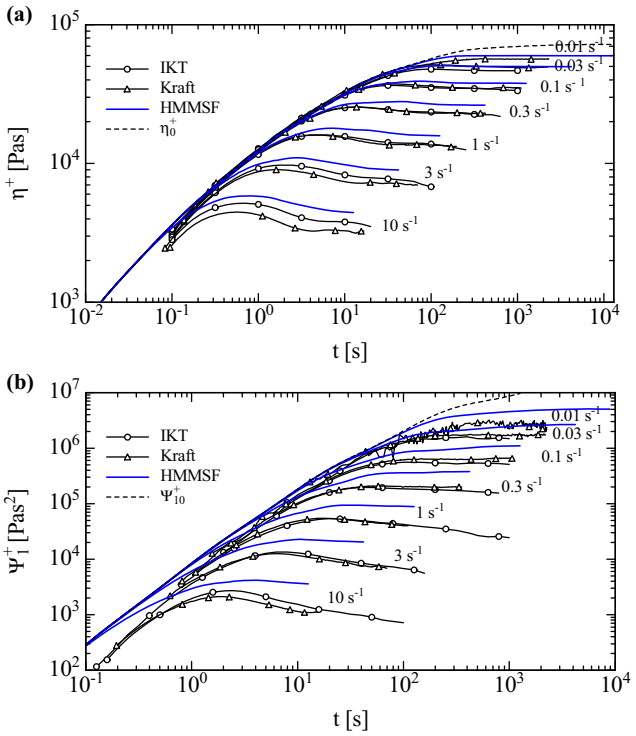

Fig. 1 Comparison of the predictions (*lines*) of the HMMSF model (Eqs. 1 and 4) with (**a**) shear viscosity and (**b**) first normal stress function data (*lines with symbols*) of an LDPE melt [Kraft ((Kraft 1996) and Bastian (Bastian 2001; Wagner et al. 2001) (IKT)] at 150 °C

800, Rheometric Scientific™) at 150 °C. The significance of these data is due to their separate measurements and reproducibility in different laboratories, i.e. the Polymer Physics Lab at ETH Zurich, Switzerland, and the IKT at Stuttgart, Germany. In the figures, the measurements at the ETH (Kraft 1996) are denoted by 'Kraft', while the measurements of Bastian (Wagner et al. 2001) are denoted by 'IKT'. We think that the differences seen between the two data sets at the higher shear rates are an honest account of the measurement accuracy that could be expected at the time.

Figure 1 shows the predictions of the start-up of steady simple shear flow of LDPE melt by the HMMSF model (Eqs. 1 and 4). The model is in qualitative agreement with the time-dependent shear viscosity data (Fig. 1a); however, the model over-predicts the shear viscosity particularly at higher strain rates. Likewise, the predictions for the first normal stress function data (Fig. 1b) demonstrate quantitative disagreements with the HMMSF model where the model over-predicts the data at all shear rates. Additionally, the model does not predict the occurrence of significant maxima at high shear rates (1–10 s^{-1}) and features only very weak maxima at large strains. The observed experimental delays in the rise-time of the first normal stress signals are due to the limited stiffness of the instrument, which causes radial inflow of the melt (Meissner 1972).

The lack of satisfactory agreement between the HMMSF model and the shear deformation data may be due to the absence of a flow-dependent phenomenon in polydisperse polymeric systems termed the convective constraint release (CCR) relaxation mechanism. In the following sections, we will discuss the incorporation of this rheological phenomenon into the HMMSF model.

Convective constraint release in shear flow

The occurrence of the convective constraint release (CCR) relaxation mechanism in polydisperse polymers was originally introduced in the tube model by Marrucci (Marrucci 1996) and Ianniruberto and Marrucci (Ianniruberto and Marrucci 1996). CCR mechanism explains that when the shear rate is significantly greater than the inverse of the longest relaxation time, topological constraints are removed due to convection caused by the flow. According to Marrucci (Marrucci 1996), during fast deformations when the neighbouring chains separate in a time order of $1/\dot{\gamma}$, the overall relaxation happens as a result of the diffusion due to Brownian thermal motion (defining linear viscoelasticity even in the absence of flow), as well as the removal of topological constraints through relative

motion among the chains by convection. Ianniruberto and Marrucci (Ianniruberto and Marrucci 1996) stated that the chains under flow exhibit an inward motion relative to their tubes, and consequently, this inward motion brings about the retraction of the chains within the tubes leading to the removal of the topological constraints for other chains. Therefore, the reptation and CCR relaxation mechanism collaborate in the renewal of the topology of entanglements, i.e. tube renewal, at high strain rates in polydisperse systems. They defined the collaborative impact of the diffusion and CCR mechanism on the overall relaxation frequency $1/\tau$ of a polydisperse polymer as (Ianniruberto and Marrucci 1996),

$$\frac{1}{\tau} = \frac{1}{\tau_0} + \beta \mathbf{K} :< \mathbf{uu} > \tag{5}$$

Here, $\frac{1}{\tau_0}$ is the diffusion renewal frequency, $\beta\mathbf{K}:<\mathbf{uu}>$ is the CCR renewal frequency, **u** depicts the Doi and Edwards (DE) segmental orientation unit vector (Doi and Edwards 1986), **K** is the velocity gradient tensor, and β is the numerical coefficient of the CCR mechanism evaluated as a fitting parameter. In a single mode toy model, they identified the diffusion relaxation time τ_0 as the reptation time.

Recently, Ianniruberto (Ianniruberto 2015) generalized this idea to the polydisperse case and formulated CCR for a multi-mode model as

$$\frac{1}{\tau_{\mathrm{iCCR}}} = \frac{1}{\tau_i} + \beta\left(\mathbf{K} : \overline{\mathbf{S}} - \frac{1}{\lambda}\frac{d\lambda}{dt}\right) \tag{6}$$

where τ_{iCCR} and τ_i are the overall orientational relaxation times, and their thermal contributions, respectively. The single-mode longest relaxation time (τ_0 in Eq. 5) is now replaced by the linear-viscoelastic relaxation times τ_i. Moreover, in the CCR part of Eq. 6, $<\boldsymbol{uu}>$ is replaced by the mean tube orientation tensor,

$$\overline{\mathbf{S}}\ (t) = \int_{-\infty}^{t} [1/\tau_d(t')]\exp\left[-\int_{t'}^{t} dt''/\tau_d(t'')\right]\mathbf{Q}(t,t')dt' \tag{7}$$

$\mathbf{Q}(t,t')$ stands for the deformation-dependent universal tensor of DE. $\lambda = L/L_{\mathrm{eq}}$ is the tube length ratio, and L_{eq} is the tube length at equilibrium. The disengagement time, τ_d, in Eq. 7 represents the mean orientational relaxation time, and at any given time

$$\tau_d(t) = \frac{\sum_i g_i \tau_{i\mathrm{CCR}}^2}{\sum_i g_i \tau_{i\mathrm{CCR}}} \tag{8}$$

The main difference between the modified CCR model of Eq. 6 and its primary version (Eq. 5) is the subtraction of the real deformation rate ($\frac{1}{\lambda}\frac{d\lambda}{dt}$) from the average deformation, $\mathbf{K} : \mathbf{S}$. However, the multi-mode version of the CCR model (Eq. 6) can cause complications in the cases of reverse flow when a sudden change of flow direction is imposed on the system, and also at high strains when the chains are aligned in the direction of flow during simple shear deformation. As seen from Eq. 6, the impact of CCR on the relaxation mechanism is dependent on three separate components, i.e. the velocity gradient tensor, the tube orientation tensor and the real deformation rate. At the moment of reverse flow, the velocity gradient and the real deformation rate instantly change direction and consequently their signs. Yet, as shown in Eq. 7, the tube orientation tensor is a function of relaxation time, and thus, it takes a significantly longer time to change its direction and sign. This inconsistency in Eq. 6 causes a decrease in CCR relaxation part, $\beta\left(\mathbf{K} : \mathbf{S} - \frac{1}{\lambda}\frac{d\lambda}{dt}\right)$, and accordingly, the overall relaxation time of the system rises, which would mean that constraints are created rather than released by convection. Moreover, similar conjectural escalation in the overall relaxation time of the system can also follow when the chains are fully aligned in the direction of shear flow, and consequently, the orientation tensor **S** tends towards zero. In other words, the CCR model in the form of Eq. 6 can create topological constraints in simple and reverse shear flows leading to prolonged relaxation mechanism, which seems to be counterintuitive.

Wagner and co-workers (Wagner et al. 2001) addressed the irreversibility of the CCR relaxation mechanism when they explained this process from a free energy perspective, i.e. dissipative CCR. They also elucidated the difference between constraint release in extensional and shear flows by introducing two unit vectors, $\boldsymbol{p}(t)$ and $\boldsymbol{q}(t)$, to describe orientation and cross-section of a tube segment. $\boldsymbol{p}(t)$ is a unit vector tangential to a tube segment at any time t, and $\boldsymbol{q}(t)$ is the unit vector normal to the tube cross-section at any time t,

$$\begin{aligned} \mathbf{p}(t) &= \frac{\mathbf{u}'}{u'} \\ \mathbf{q}(t) &= \frac{\mathbf{n}'}{n'} = \mathbf{p}(t) \end{aligned} \tag{9}$$

Here, u' and n' are the lengths of the deformed unit vector $\mathbf{u}'$, and affinely deformed surface vector $\mathbf{n}'$ (Wagner et al. 2001), respectively.

The convective time derivatives of $\mathbf{p}(t)$ and $\mathbf{q}(t)$,

$$\begin{cases} \overline{\mathbf{p}}\ (t) = \mathbf{K}.\mathbf{p}(t) = \dfrac{1}{u'}\dfrac{\partial \mathbf{u}'}{\partial t} \\ \overline{\mathbf{q}}\ (t) = -\mathbf{K}^T.\mathbf{q}(t) = \dfrac{1}{n'}\dfrac{\partial \mathbf{n}'}{\partial t} \end{cases} \tag{10}$$

represent the affine rates of change in the segmental tube orientation vector and the tube cross-sectional area vector, respectively. Wagner et al. (Wagner et al. 2001) demonstrated a schematic display of $\mathbf{q}(t)$ and $\mathbf{p}(t)$ during extensional and

simple shear flows. As shown in Fig. 2, $\mathbf{q}(t)$ and $\mathbf{p}(t)$ are always coaxial (anti-parallel) in non-rotational (extensional) flows, while they are always perpendicular in shear (rotational) flows.

As schematically depicted in Fig. 3, the coaxiality of $\mathbf{q}(t)$ and $\mathbf{p}(t)$ during extensional deformation leads to the compensation of any constraint release effects by the advection of the neighbouring topological constraints in the direction of flow (Fig. 3a), and hence results in a minimum tube diameter and a maximum molecular stress function, $f_{\max}$ (Wagner et al. 2000, 2001), under steady-state conditions. On the other hand in shear flow, when the tube segment is aligned in the flow direction at high shear strains, the affine change in tube segment length due to convection tends towards zero. However, the affine change in tube cross-sectional area continues (Fig. 3b), and topological constraints above and below the chain are released, and the tube diameter returns to its equilibrium value a_0. Therefore, while CCR has no effect in extensional flows, it is indispensable to incorporate a dissipative CCR mechanism at higher shear strains into the HMMSF model.

We therefore introduce a constraint release (CR) term, modifying the relaxation times τ_i in the evolution Eq. 4 of the molecular stress function,

$$\frac{1}{\tau_{i\mathrm{CR}}} = \frac{1}{\tau_i} + \beta CR \tag{11}$$

and therefore Eq. 4 is now given by

$$\frac{\partial f_i}{\partial t} = f_i(\mathbf{K}:\mathbf{S}) - \frac{f_i - 1}{\tau_{i\mathrm{CR}}}\left(1 - \frac{2}{3}w_i^2\right) - \frac{2}{3}\frac{f_i^2\left(f_i^3 - 1\right)}{3\tau_{i\mathrm{CR}}}w_i^2 \tag{12}$$

with $\tau_{i\mathrm{CR}}$ from Eq. 11. Regarding the formulation of the CR term, which shall be only active in rotational (shear) flows and shall obey the condition of irreversibility, we follow Wagner et al. (Wagner et al. 2001) by expressing CR in Eq. 12 as,

$$\mathrm{CR} = \frac{1}{2}\sqrt{\left|\left\langle\left(\overline{\mathbf{q}}\,.\overline{\mathbf{q}} - \overline{\mathbf{p}}\,.\overline{\mathbf{p}}\right)\right\rangle\right|} = \sqrt{|\mathbf{W}.\mathbf{D}:\mathbf{S}|} \tag{13}$$

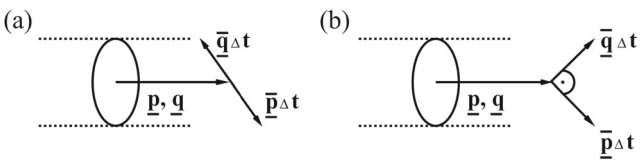

Fig. 2 Schematic representation of the affine rates of change of the tube segment orientation vector **p** and of the cross-sectional surface vector **q**, in the case of (**a**) extensional flow and (**b**) simple shear flow. **q** and **p** are always coaxial in non-rotational flows, while they are always perpendicular in shear flow (Bastian 2001)

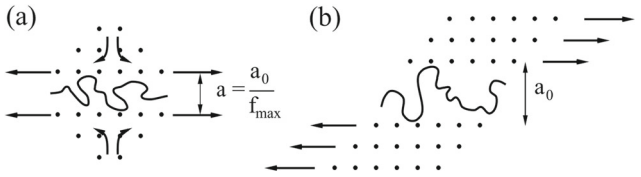

Fig. 3 (**a**) In extensional flow and large strains, any constraint release effects are compensated by the advection of neighbouring topological constraints, leading to a minimum tube diameter a and a maximum molecular stress $f_{\max}$. (**b**) In shear flow and large strains, the molecule is simply oriented in the flow direction and, due to convective constraint release above and below the molecular chain, the tube diameter returns to its equilibrium value a_0 (Bastian 2001)

with

$$\mathbf{D} = \frac{1}{2}\left(\mathbf{K} + \mathbf{K}^T\right) \tag{14}$$

$$\mathbf{W} = \frac{1}{2}\left(\mathbf{K} - \mathbf{K}^T\right) \tag{15}$$

D is the rate of deformation tensor, and **W** the rate of rotation tensor.

Alternatively, for steady shear flows, Eq. 13 can be expressed in terms of the second order Rivlin-Ericksen tensors $\mathbf{A}_1$ and $\mathbf{A}_2$,

$$\begin{aligned}\mathbf{A}_1^2 &= 4\mathbf{D}^2\\ \mathbf{A}_2 &= \mathbf{A}_1^2 + 2\left(\mathbf{W}.\mathbf{D} + \mathbf{D}.\mathbf{W}^T\right)\end{aligned} \tag{16}$$

resulting in

$$\mathrm{CR} = \frac{1}{2}\sqrt{\left|\mathbf{A}_2:\mathbf{S} - \mathbf{A}_1^2:\mathbf{S}\right|} \tag{17}$$

It is obvious from Eqs. 16 and 17 that CR is identical to zero in irrotational (extensional) flows, while in simple shear flows, CR is given by

$$\mathrm{CR} = \frac{1}{2}\sqrt{\dot{\gamma}^2|S_{11} - S_{22}|} \tag{18}$$

The HMMSF model with evolution Eq. 12 can now be used to predict the overall rheological behaviours of LCB polymers in both simple steady, and reverse shear deformations with only two non-linear parameters, i.e. G_{D} (dilution modulus) and β (CR parameter).

Comparison between HMMSF model predictions including CCR term and experimental shear data

We start by presenting predictions of a multi-mode equivalent of the CCR model of Ianniruberto and Marrucci (Ianniruberto and Marrucci 1996) (Eq. 5) for LDPE melt, i.e. we display in

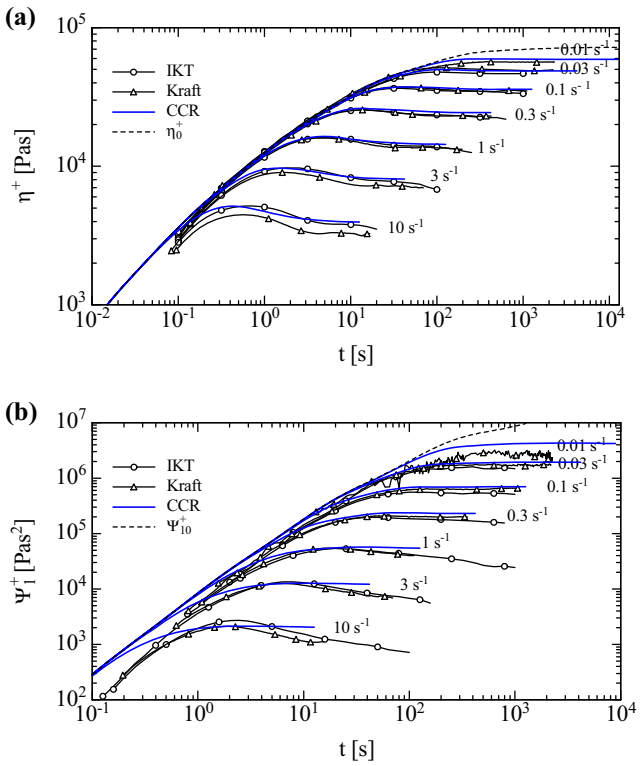

Fig. 4 Comparison of the predictions (*blue lines*) of a multi-mode equivalent of the CCR model of Ianniruberto and Marrucci (Ianniruberto and Marrucci 1996) (Eq. 5 with β = 0.5) with (**a**) shear viscosity and (**b**) first normal stress function data (*lines with symbols*) of an LDPE melt [Kraft (Kraft 1996) and Bastian (Bastian 2001; Wagner et al. 2001) (IKT)] at 150 °C

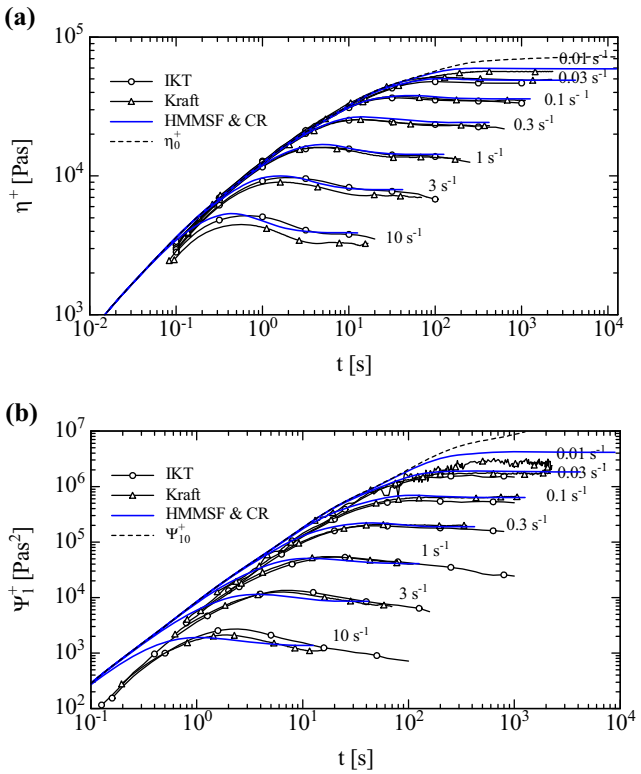

Fig. 5 Comparison of the predictions (*blue lines*) of the HMMSF model including the CR term (Eqs. 1, 11, 12 and 17 with β = 0.14) for LCB melts with (**a**) shear viscosity and (**b**) first normal stress function data (*lines with symbols*) of an LDPE melt [Kraft (Kraft 1996) and Bastian (Bastian 2001; Wagner et al. 2001) (IKT)] at 150 °C

Fig. 4 the predictions of the HMMSF model (Eqs. 1, 11 and 12) with a CR term of

$$\mathrm{CR} = \mathbf{K} : \mathbf{S} = \dot{\gamma} S_{12} \tag{19}$$

The selection of this CR term in Eq. 11 with a CCR coefficient of β = 0.5 leads to good agreements with the shear viscosity data (Fig. 4a). However, the predictions of this model for the first normal stress function are not in good accordance with the data (Fig. 4b) as no maxima are predicted. We also attempted to model the shear data by the equivalent of the modified CCR model of Ianniruberto (Ianniruberto 2015) (Eqs. 6), i.e. applying a CR term of

$$\mathrm{CR} = \mathbf{K} : \mathbf{S} - \frac{1}{f_i}\frac{\partial f_i}{\partial t} \tag{20}$$

However, the CR term of that model becomes negative when the second term on the right hand side becomes larger than **K**:**S**, which even leads to negative effective stretch relaxation times.

Figure 5 displays the comparison between the predictions of the HMMSF model (Eqs. 1, 11 and 17) with a CR term according to Eq. 18 and the shear data. A constraint release parameter β = *0.14* leads to good agreement of predictions with the shear data for both low and high shear rate deformations. The prediction of the maxima of the first normal stress function is in good accordance with the observed maxima particularly at high shear rates (Fig. 5b). However, the incidence of the experimental delay of the rise-time prevents a direct comparison between our model and the data. In Fig. 6, we have therefore shifted the predictions of the model at high shear rates in time to mimic the experimental delays of the instrument.

Overall, the modified HMMSF model provides a promising realization of shear flow behaviour of LCB polymers, while not compromising the excellent prediction of extensional flows as demonstrated in parts I and II of this series (Narimissa et al. 2015, 2016).

Conclusions

The hierarchical multi-mode molecular stress function (HMMSF) model for long-chain branched (LCB) polymer melts implements the basic ideas of (i) the pom-pom model, (ii) hierarchal relaxation, (iii) dynamic dilution and (iv) inter-chain pressure. It is based on the assumption that stretch and

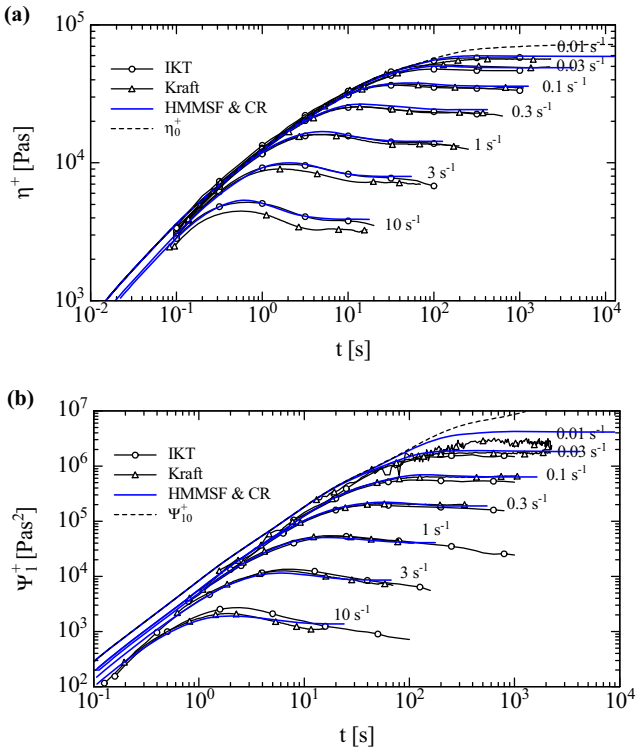

Fig. 6 Comparison of the predictions (*blue lines*) of the HMMSF model including the CR term (Eqs. 1, 11, 12 and 17 with $\beta = 0.14$) for LCB melts with (**a**) shear viscosity and (**b**) first normal stress functin data (lines with symbols) of an LDPE melt [Kraft (Kraft 1996) and Bastian (Bastian 2001; Wagner et al. 2001) (IKT)] at 150 °C. The predictions of higher rates are shifted in time: (**a**) by a factor of 1.3 and 1.4 for shear rates 3 and 10s^{-1}, respectively; (**b**) by a factor of 1.3, 1.4, 1.6 and 1.9 for shear rates 0.3, 1, 3 and 10 s^{-1}, respectively) to mimic the experimental delay of the stress signal due to limited stiffness of the rheometer

orientation are coupled, and stretch is implemented through a tube diameter which decreases with increasing deformation. Therefore, stretch and orientation of tube segments have the same dynamics as characterized by the linear-viscoelastic relaxation spectrum. The HMMSF model, with only one free non-linear parameter, namely the dilution modulus G_D, is able to model the extensional viscosity data of broadly distributed long-chain branched polymer melts in uniaxial, equibiaxial and planar deformation modes (Narimissa et al. 2015, 2016). However, this model in its original version is not capable of providing a satisfactory prediction of the shear flow behaviour of LCB melts at higher shear rates. Therefore, we incorporated a convective constraint release (CCR) mechanism into this model, which reduces chain stretch at larger shear deformations and shear rates. We argue that CCR is only important in the case of shear flows, and we implemented CCR in the evolution equation of the molecular stress function by use of a specific combination of the second order Rivlin-Ericksen tensors in such way that CCR is only active in shear flows. In this way, we also avoided the hypothetical creation of constraints (i.e. a negative CCR) after the alignment of the chains in the direction of shear flow at high strains, and also in the case of reverse flows, which is occurring in other formulations of CCR. The modified HMMSF model, with only two free non-linear material parameters, namely the dilution modulus G_D and the constraint release parameter β, is effectively capable of modelling the shear data of a broadly distributed long-chain branched polymer melt at all shear rates investigated, without compromising the excellent agreement of the HMMSF model with extensional viscosity data.

References

Bastian H (2001) Non-linear viscoelasticity of linear and long-chain-branched polymer melts in shear and extensional flows. Universität Stuttgart

Dealy JM, Larson RG (2006) Structure and rheology of molten polymers—from structure to flow behavior and back again. Hanser Publishers, Munich

Doi M, Edwards SF (1986) The theory of polymer dynamics. Oxford University Press, Oxford

Ianniruberto G (2015) Quantitative appraisal of a new CCR model for entangled linear polymers. J Rheology 59:211–235. doi:10.1122/1.4903495

Ianniruberto G, Marrucci G (1996) On compatibility of the Cox-Merz rule with the model of Doi and Edwards. J Non-Newtonian Fluid Mech 65:241–246. doi:10.1016/0377–0257(96)01,433–4

Kraft M (1996) Untersuchungen zur scherinduzierten rheologischen Anisotropie von verschiedenen Polyethylen-Schmelzen. Diss Techn Wiss, ETH Zürich

Marrucci G (1996) Dynamics of entanglements: a non-linear model consistent with the Cox-Merz rule. J Non-Newtonian Fluid Mech 62: 279–289. doi:10.1016/0377–0257(95)01,407–1

Meissner J (1972) Modifications of the Weissenberg rheogoniometer for measurement of transient rheological properties of molten polyethylene under shear. Comparison with tensile data. J App Poly Sci 16: 2877–2899. doi:10.1002/app.1972.070161114

Narimissa E, Rolón-Garrido VH, Wagner MH (2015) A hierarchical multi-mode MSF model for long-chain branched polymer melts part I: elongational flow. Rheol Acta 54:779–791. doi:10.1007/s00397–015–0879-2

Narimissa E, Rolón-Garrido VH, Wagner MH (2016) A hierarchical multi-mode MSF model for long-chain branched polymer melts part II: multiaxial extensional flows. Rheol Acta 55:327–333. doi:10.1007/s00397–016-0922-y

Wagner MH, Bastian H, Hachmann P, Meissner J, Kurzbeck S, Münstedt H, Langouche F (2000) The strain-hardening behaviour of linear and long-chain-branched polyolefin melts in extensional flows. Rheol Acta 39:97–109. doi:10.1007/s003970050010

Wagner MH, Rubio P, Bastian H (2001) The molecular stress function model for polydisperse polymer melts with dissipative convective constraint release. J Rheology 45:1387–1412. doi:10.1122/1.1413503